Desalination and Water Treatment
www.deswater.com

doi: 10.5004/dwt.2018.22510

121 (2018) 291–304
July

Chemically enhanced coffee husks as biosorbents for the removal of copper and nickel ions from aqueous solutions: study on kinetic parameters

J. Arun[a], R. Sushma[b], B.S. Darshan[b], M. Pandimadevi[b,*]

[a]*Department of Chemical Engineering, SSN College of Engineering, Chennai 603110, India*
[b]*Department of Biotechnology, School of Bioengineering, SRM Institute of Science and Technology, Kattankulathur, Chennai 603203, India, Tel. +91 9444145987; email: pandimadevi2008@gmail.com (M. Pandimadevi)*

Received 21 March 2018; Accepted 15 May 2018

ABSTRACT

Biosorption of Cu and Ni ions onto low-cost coffee husk (CH) was investigated in this study. Adsorbent was activated using $ZnCl_2$, and the desorption studies revealed the increase in adsorption with high regeneration capacity. Adsorbent was characterized by Fourier-transform infrared and its point of zero charge was determined using pH drift method. Effects of pH, reaction time, and adsorbent concentration on metal ions adsorption were studied. Physical modification of adsorbent at varying temperature 37°C to 90°C depicted that the temperature was inversely proportional to adsorption efficiency. Study parameters showed that pH 6, temperature 37°C, and reaction time 6th hour (for copper) and 10th hour (for nickel) exhibited maximum efficiency. The equilibrium adsorption data were analyzed using Langmuir, Freundlich, Redlich, and Sips adsorption isotherms with Langmuir providing a best fit ($R^2 > 0.96$). Immobilization studies were carried by encapsulating CHs in alginate beads, and the experiment was carried out for both batch and continuous modes, where the continuous modes were carried out using a column apparatus. Both batch and continuous studies showed 95% efficiency in removal of heavy metals. From these studies, it is clear that CHs are better low-cost adsorbents of heavy metals from aqueous solutions.

Keywords: Coffee husk; Copper; Nickel; FT-IR; Langmuir and Freundlich isotherm

1. Introduction

Applications of heavy metals are endless; nickel is used in cadmium–nickel rechargeable batteries and copper is widely used in electrical appliance. Among various heavy metals, Pb(II), Ni(II), and Cr(VI) ions are deemed to be highly toxic [1,2]. These metals are directly and indirectly exposed to aquatic food chain and enters aquatic ecosystem and terrestrial system [3,4]. Continuous accumulation of these toxicants in running and drinking water source causes various health issues. Exposure to arsenic leads to skin cancer and skin lesions such as hyperkeratosis and pigmentation changes; cadmium exposure may cause renal failure; mercury poisoning damages the central nervous systems and can lead to a disorder known as "mad-hatter" disease; exposure to copper can lead to Wilson's disease, if the toxicity level exceeds 1 mg/L; and nickel is known to cause various skin allergies [5]. Long-term exposure of humans to nickel, chromium, and lead leads to cancer, asthma, respiratory diseases, skin cancer, kidney disorder, nerve damage, and bone disorder [1,2,6].

Current techniques to remove heavy metals from industrial effluents include reverse osmosis, membrane filtration, electrodialysis, and photocatalysis [7–10]. Although their efficiencies in removing the heavy metals are appreciable, these processes incur other expenses such as exorbitant capital cost, operational costs, and maintenance cost, which is not

* Corresponding author.

Presented at the 3rd International Conference on Recent Advancements in Chemical, Environmental and Energy Engineering, 15–16 February, Chennai, India, 2018

1944-3994/1944-3986 © 2018 Desalination Publications. All rights reserved.

economical. Recently, cation exchange-based polyaniline silicate, nitrogen-doped mesoporous carbon, multiwall carbon nanotubes/ThO_2 nanocomposites, sodium dodecyl sulfate-supported nanocomposites-based cation exchanger, and metal–organic framework-based composites were efficient in heavy metals (cadmium and nickel), Ph(II), Cu^{2+}, and U(VI) and Th(IV) ions adsorption from aqueous medium [11–15]. Membrane-based separation is the expensive technique in effluent treatment operation, but heavy metals with higher specific density greater than 5 g/m^3 are easy to separate [5].

Adsorption is considered to be quite attractive method in terms of its efficiency, in removing the heavy metals even from aqueous solutions [16,17]. Although, there are commercial adsorbents such as activated carbon, chitosan, zeolite, and clay are popularly used due to their high adsorption properties. Recently, new adsorbents were prepared from agricultural waste for the effective adsorption of Pb(II) from aqueous solutions [18]. Agriculture waste-based activated carbon was framed for effective removal of BrO^{3-} from water medium [19].

Coffee is one among the most commonly preferred and consumed beverages throughout the world. The world's annual demand of coffee seeds reached 7 million tons. This process generates huge amount of by-products and waste according to International Coffee Organization [20]. Coffee husk (CH) was one of the major by-products coming out of the coffee roasting and processing. During this process, coffee skin undergoes structural and chemical changes leading to fragmentations [21]. CH can be used as cheap adsorbent for removal of pollutants from wastewater. For example, untreated CHs can act as effective adsorbent of cadmium ions [22]. Similarly, Baek et al. [23] revealed that the degreased green coffee beans can be used as effective adsorbents for the removal of malachite green from aqueous solutions. Alginate was a heteropolysaccharide of β-D-mannuronic acid and α-L-guluronic acid widely used for uptake of metal ions from water with higher selectivity due to formation of cross-linked stable gel [24].

An ideal adsorbent should have high adsorption capacity, good selectivity, and easy regenerability. Thus, there is an increasing demand for relatively low-cost, efficient, and easily available adsorbents for the adsorption of heavy metals. In this study, we have enhanced and modified the properties of CH, and the kinetic parameters on the biosorption of heavy metals such as copper and nickel from industrial effluent were studied.

2. Materials and methods

2.1. Collection and preparation of biosorbent

CHs were collected from local coffee manufacturer (Babu coffee seeds) Chennai, Tamilnadu, India. The collected CHs were ground into fine particles and sieved into 0.5 mm particles and were used as adsorbent throughout the study. To arrest chemical modification, CH powders were stored in an airtight container. All reagents used were of analytical grade without further purification. The adsorption of heavy metal ions using low-cost adsorbents was evaluated under various conditions such as pH, heavy metal concentration, and adsorbent dose through both kinetic and isotherm studies.

2.2. Preparation of metal ion solution

Copper and nickel ions solutions were prepared using $CuSO_4.5H_2O$ and $NiSO_4.7H_2O$, respectively. Stock solutions were prepared by dissolving known quantity (1 g/L) of salts in distilled water. The working solutions were prepared by diluting the stock solution using distilled water.

2.3. Biosorbent modification studies

Chemical modification of activated carbon was done by treating the acidic and basic reagents such as 0.1 M of HNO_3, KOH, and $ZnCl_2$, respectively, to remove copper ions form the solution. Similarly, another set of experiments carried out in Erlenmeyer conical flasks with reagents such as 0.1 M of HNO_3, KOH, and $ZnCl_2$, respectively, to treat activated carbon from CH for removal of nickel ions from the solution. The experiments were carried out in batch process. The chemically treated samples were subjected to 100 mg/L working standards for 2, 4, 6, 8 h for copper and nickel, respectively. Later, the concentration of copper and nickel in the filtrate were analyzed using atomic adsorption spectroscopy (AAS) (SL-176 model, Elico, Chennai, India).

2.4. Characterization studies

Interaction between the chemical bonds and the metal ions on the surface of the adsorbent material was examined using Fourier-transform infrared (FT-IR) instrument (PerkinElmer 200 FTIR, USA) within the range of 400–4,000 cm^{-1}. Samples of nonactivated CH and activated with HNO_3, KOH, and $ZnCl_2$ were analyzed. The pH of the solution was measured using pH meter equipped with combined glass electrode. Point of zero charge (PZC) measurement provides data for predicting the ionic nature of the catalyst, which helps in determining the mechanism of dye–catalyst interaction. If PZC is at particular pH, the surface charge of the sample is found to be neutral. The PZC value was found by using pH drift method. A total of 0.05 M of NaCl solution was prepared with five different pH (2, 4, 6, 8, and 10), and 50 mL of 0.05 M of NaCl solution was taken in a 250 mL conical flask and pH was adjusted by using 0.1 M of HCl or 0.1 M of NaOH. A total of 100 mg of untreated CH was added to the conical flasks, and the solution was incubated at 37°C for 48 h in orbital shaker at 150 rpm at room temperature. After 48 h. the solutions were taken and PZC was calibrated. Parameters such as pH, contact time, and adsorbent dosage were calculated using batch adsorption experiments.

2.5. Adsorption batch studies

2.5.1. Effect of initial ion concentration

Effect of initial ion concentration on adsorption efficiency was studied through batch studies. The working solution was prepared by diluting stock solution into desired concentrations (25–150 mg/mL). The chemically modified adsorbents were used to adsorb metal ions from the solution. The pH of the solution was adjusted using 0.1 M of HCl and 0.1 M of NaOH solution. The metal ion concentration before and after adsorption studies was analyzed using AAS (SL-176 model, Elico).

2.5.2. Effect of pH and contact time

Adsorption efficiency of the adsorbate was examined by conducting batch adsorption experiment to calculate the percentage removal efficiency (%) of copper and nickel ions. pH of the solution was varied from 5 to 8 by using 0.1 M of HCl and 0.1 M of NaOH for time intervals of 2–12 h. The metal solution concentration was kept constant at 75 mg/L. A known amount of adsorbent (100 mg) was added to the solution in an Erlenmeyer flask, and the flasks were stirred continuously in an orbital shaker at 150 rpm for the specified time intervals in a temperature-controlled environment. Finally, the solutions were filtered and the filtrate was analyzed using AAS. The measured data from the batch adsorption process were used to calculate the percentage removal efficiency of metal ions by using Eq. (1):

$$\text{Efficiency } \% = \frac{C_o - C_e}{C_o} \times 100 \tag{1}$$

where C_o is initial equilibrium concentration (mg/L) and C_e is final equilibrium concentration (mg/L) of metal ions in the solution.

2.5.3. Effect of adsorbent dosage

The experiments to find the effect of adsorbent concentration were carried out by shaking the known concentration of metal ion solution with varying adsorbent dosage in an Erlenmeyer conical flask at room temperature. The metal solutions (75 mg/L) were prepared and adjusted to the optimum pH of 7 using 0.1 M of HCl or 0.1 M of NaOH solutions. The adsorbent dosage was varied from 100 to 500 mg/100 mL. The solution was mixed for the optimum contact time at 150 rpm. The solutions were filtered and, the filtrate was analyzed using AAS. The measured data from the batch process were used to calculate the percentage removal efficiency of metal ions by using the above Eq. (1)

2.5.4. Effect of temperature

The batch experiments were carried out at different temperatures such as 25°C, 30°C, 35°C, 40°C, 45°C, 50°C, and 55°C, respectively, for the known concentration of ion solutions. Initially, 75 mg/L concentration of standard metal ion solution was prepared in three different 250 mL Erlenmeyer conical flasks, the other parameters are pH 7 and contact time 6 h for copper and pH 7 and contact time 8 h for nickel. A total of 100 mg of CH was added and incubated along with the metal ion solution and continuously shaked for 2 h in 150 rpm. Then the solution was filtered, and the filtrate was collected to find metal adsorption on CH surface by using AAS.

2.6. Desorption studies

In this method, the spent adsorbent was washed with three different desorbing agents. In this study, 0.1 M of HCl, 0.1 M of NaOH, and deionized water were used as desorbing agents. A total of 1 g of sample was added in 100 mL of desorbing agent and agitated for 30 min at room temperature. Then the adsorbent was filtered out, oven dried, and used for next cycle of adsorption experiments. The effluent concentration was analyzed using AAS. The percentage of desorption was calculated using Eq. (2):

$$\text{Desorption } (\%) = \frac{\text{Final metal concentration}}{\text{Initial sorbed concentration}} \times 100 \tag{2}$$

2.7. Recycling studies on spent adsorbent

To study the effect of recyclability nature of spent adsorbent, the spent adsorbent was subjected to consecutive batch adsorption studies. Around 100 mg of adsorbent was added to 75 mg/L concentration of standard metal ion solution in a 250 mL Erlenmeyer conical flask with other parameters like pH 7 and contact time 6 h for copper and pH 7 and contact time 8 h for nickel. Then the adsorbent was filtered out, oven dried, and used for next cycle of adsorption experiments. The effluent concentration was analyzed using AAS. The removal percentage of metal ions was calculated using the above Eq. (1).

2.8. Adsorption isotherms

A series of different concentrations of ion solutions were prepared and batch adsorption studies were done to analyze the Langmuir, Freundlich, Redlich–Peterson, and Sips isotherms under specific conditions: initial pH of 7, adsorbent dosage of 1 g/L, contact time of 30 min, and ion concentration of 75 mg/L. After the experiment, the ion concentration in the solution is analyzed by AAS. The quantity of metal ions adsorbed by adsorbent at equilibrium condition, q_e (mg/g), was estimated using Eq. (3):

$$q_e = \frac{(C_o - C_e)}{m} \times V \tag{3}$$

where q_e is the adsorption capacity at equilibrium (mg/g), V is the volume of metal ions solution (g), C_o is the initial concentration of metal ions (mg/L), C_e is the equilibrium concentration of metal ions (mg/L) in the solution, and m is the biosorbent dosage (g).

The two parameters (Langmuir and Freundlich) and three parameters (Redlich–Peterson and Sips) adsorption isotherm models have been adopted to fit the adsorption equilibrium data. The nonlinear regression analysis was performed to calculate the parameters such as R^2 and error values using MATLAB (R) curve fitting tool. The isotherms can be expressed in an equation as follows:

Freundlich equation:

$$q_e = K_F C_e^{\frac{1}{n}} \tag{4}$$

Langmuir equation:

$$q_e = q_{\max}(K_L C_e)(1 + K_L C_e) \tag{5}$$

Redlich–Peterson equation:

$$q_e = K_{RP}C_e/(1 + \alpha_{RF}C_e\beta^{RP}) \quad (6)$$

Sips equation:

$$q_e = K_S C_e^{\beta e}/(1 + \alpha_S C_e^{1/\beta s}) \quad (7)$$

where C_e is equilibrium concentration (mg/L), C_o is initial metal ion concentrations (mg/L), K_F is characteristic constant related to the adsorption capacity (mg/g), K_L is sorption equilibrium constant (L/mg), K_{RP} is Redlich–Peterson isotherm constant (L/g), K_s is Sips model isotherm constant (L/g), n is characteristic constant related to adsorption intensity or degree of favorability, q_e is amount of solute adsorbed at equilibrium condition (mg/g),and q_{max} is saturated monolayer adsorption capacity (mg/g).

2.9. Adsorption kinetics

The adsorption kinetic experiments were performed in 100 mL Erlenmeyer conical flasks with varying metal ion concentration (25, 50, 75, 100, 125, and 150 mg/L) with adsorbent (100 mg) at a different contact time from 0 to 120 min and pH 7. The flasks were placed in a temperature-controlled shaking incubator at temperature 25°C. When equilibrium was attained, flasks were withdrawn from the shaker, and metal ion concentration was analyzed using AAS. The adsorption isotherm experimental data were used to determine the rate of adsorption and the rate-controlling mechanism of the metal ions removed from aqueous solution. The experimental data were fitted with pseudo-first-order, pseudo-second-order, Elovich kinetic, and Weber kinetic models. The linear regression analysis was carried out to examine the adsorption kinetic parameters, R^2 and error values using MATLAB (R) curve fitting tool.

2.10. Immobilization of adsorbent and packed column studies

The primary reason for this can be attributed to their easy availability, cost, environmentally benign nature, biodegradability, and renewability. Such beads generally provide three-dimensional support to the adsorbent. The immobilized heterogeneous adsorbent possesses effective surface area for the reaction. The activity of free and immobilized adsorbents was initially carried out in a 75 mg/L of metal ion concentration solution individually.

2.10.1. Calcium alginate immobilization

Immobilized beads were prepared using 3% sodium alginate solution dropped in to 0.2 M of $CaCl_2$ solution. About 1 g of activated CH ($ZnCl_2$) was added in 50 mL of sodium alginate solution along with 20 mL of 4% gluteraldehyde solution to form cross linkage, and beads were prepared. For control studies, empty beads were prepared without addition of adsorbent.

2.10.2. Hybrid immobilization

The hybrid beads consisted of silica–calcium alginate combined with CH as adsorbent and gluteraldehyde as crosslinker. A total of 20 g of silica was added to 60 mL of distilled water and heated at 80°C to form silica slurry. In total, 3% sodium alginate solution was prepared and stirred with the silica slurry for 30 min. A total of 1 g of CH was added to the mixture along with 4% gluteraldehyde, and beads were prepared.

2.10.3. Column studies

Continuous flow adsorption experiments were carried out in a glass column apparatus. Column used for the study had an internal diameter of 3 cm and height of 30 cm. The prepared beads were filled to the varying heights (10, 15, 20, and 25 cm) of the column. The flow rate was maintained at 10 mL/min. The metal ion solution of known concentration was prepared and pumped into the column upward at a desired flow rate using a peristaltic pump (PP40, Miclins, India). The effluent flow to the column was carried until zero adsorption is noted. Samples were drawn at regular time intervals and analyzed using AAS.

3. Results and discussions

3.1. Characterization studies

3.1.1. FT-IR analysis

The adsorption characteristics of adsorbent fully depend upon the chemical reactivity of functional groups present on the surface. The functional groups such as carboxyl, hydroxyl, and amine groups were capable for adsorbing the metal ions from the aqueous solutions. FT-IR is an important tool which analyzes the functional groups present in the surface of the adsorbent and interaction between metal ion and surface of adsorbent. Table 1 elaborates the functional groups present in both nonactivated and activated CHs.

Table 1
FT-IR spectrum of activated and nonactivated coffee husk

Sample mode	Stretching	Functional groups
Nonactivated coffee husk	2,923 cm^{-1}	Methyl groups
	1,641.73 cm^{-1}	C–H stretching
	1,063 cm^{-1}	Esters
	1,428.51 cm^{-1}	C–H bending of CH_3
Coffee husk activated by HNO_3	3,426.101 cm^{-1}	Hydroxyl groups
	2,921.84 cm^{-1}	C–H stretching
Coffee husk activated by HCl	3,416.09 cm^{-1}	NH stretching
	1,058.32 cm^{-1}	Silicon groups
Coffee husk activated by $ZnCl_2$	3,422 cm^{-1}	O–H stretching
	2,921 cm^{-1}	C–H alkane groups
	1,049 cm^{-1}	C=S stretching
Coffee husk activated by KOH	2,919.47 cm^{-1}	Alkenes
	1,057.44 cm^{-1}	Si-H vibrations
Coffee husk activated by NaOH	2,919.30 cm^{-1}	Alkenes
	1,033.74 cm^{-1}	Halogenic compounds

The functional groups in the adsorbent surface illustrate the presence of carboxylate, amino, alkane, alcoholic, and hydroxyl groups were interacted with protons or metal ions. The results confirmed that the CH has more potential adsorption capacities for the removal of nickel and copper ions from aqueous solutions.

3.1.2. Determination of PZC

The net particular charge around the surface zero is called the point of zero charge, which is one of the most important parameters to describe the surface charge properties of an adsorbent. Several methods such as mass titrations, potentiometric titrations, salt addition methods, etc. have been published to determine the PZC of an adsorbent, out of which, the pH drift method offers various advantages. The addition of adsorbent will induce a shift in the pH of the solution in the direction of PZC. The pH at which the addition of adsorbent does not induce a shift in the pH is determined to be its PZC.

From Fig. S1, it can be identified that the PZC of CH lies at a pH value of 7.08. This is a neutral pH range. The parameter studies showed an optimum pH range around neutral to alkaline range too. This may indicate that because metal ions are cationic and the surface of CH is negatively charged, effective adsorption is taking place as the metal cations are attracted to the surface of the adsorbent. This helps in understanding the principle of adsorption process and reveals why adsorption process is pH sensitive.

3.1.3. Adsorbent modification studies

The surface of the adsorbent was activated using various chemical agents to study the effect of modifications on adsorption. The aim of the modification was to reduce the contact time between the adsorbent and adsorbate, so that maximum efficiency could be reached at a shorter period. The following chemical agents were used for the activation: HNO_3 (acid), $ZnCl_2$ (salt), and KOH (base). The effect of modification by these agents is depicted in Fig. 1.

From Fig. 1, it can be interpreted that as contact time increases, the efficiency of copper adsorption increases, stating that the surface-activated adsorbent is showing promising results. The nonactivated adsorbent is showing maximum efficiency of 87.6% at 8 h, while the adsorbent which was activated with HNO_3 shows 78.5% at 2 h and 92.4% at 8 h; with KOH shows 80.61% at 2 h and 96.57% at 6 h; and with $ZnCl_2$ shows 86.2% in 2 h and 99.16% at 6 h. Because the activating agent, $ZnCl_2$, gave an efficiency value of 99.16% at 6 h itself, it was chosen to be a better modifying agent when compared with acids and bases.

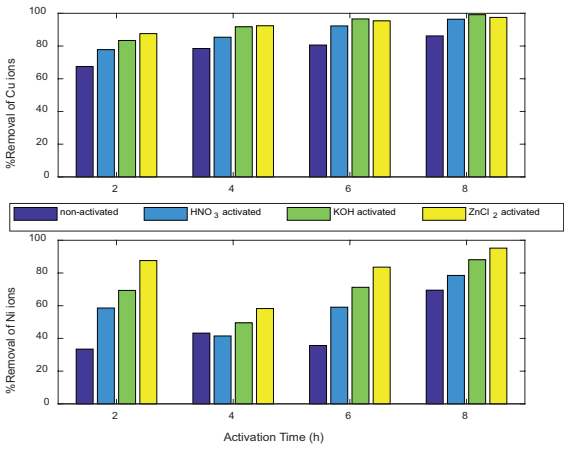

Fig. 1. Effect of activating agents on copper and nickel ion adsorption.

The following chemical agents were used for the activation: HNO_3 (acid), $ZnCl_2$ (salt), and KOH (base). The effect of modification by these agents on nickel adsorption is depicted in Fig. 1. It was identified that $ZnCl_2$ is a better modifying agent, which shows efficiency values of 95.23% at 8 h, while the nonactivated adsorbent shows maximum efficiency of only 87.59% at 8 h. The maximum efficiency value for HNO_3-activated sample is 58.26% at 8 h while that of KOH is 83.58% at 8 h. These values are relatively lower when compared with $ZnCl_2$-activated sample, thus proving that $ZnCl_2$-activated CH as an important adsorbate on nickel adsorption.

The adsorption activity of biosorbent depends upon the chemical reactivity of the functional groups present at the surface. FT-IR analysis was done to identify the functional groups such as carboxyl, hydroxyl, and amine groups because they were capable of adsorbing metal ions. The interaction between the metal ions and the chemical bonds on surface of adsorbent revealed the functional groups and their corresponding stretching vibrations. The vibration at 3,349 cm^{-1} corresponds to O–H carboxylic acid vibration which would be attributed due to water and alcohol molecule. The vibration at 1,634 and 1,554 cm^{-1} is due to N=H amine and C–H stretching vibrations. The sorbent after adsorption was analyzed, and the results revealed that the vibration at 3,355 cm^{-1} corresponds to O–H carboxylic acid vibration which would be attributed due to water and alcohol molecule. The vibrations in between 2,860 and 2,959 cm^{-1} would be due to alkyl groups. The vibration at 1,639–1,459 cm^{-1} is due to N=H amine and C–H stretching vibrations. The results revealed that the biosorbent possessed potential adsorption capacity on metal ion removal from water solutions.

3.2. Adsorption parameter studies

The adsorption effects of heavy metals on activated CH were studied using pH, contact time, temperature, and adsorbent dosage on the husk surface.

3.2.1. Effect of initial ion concentration

The effect of initial metal (copper and nickel) ions concentration on adsorption capacity of different activated CH in range of 25–150 mg/mL of metal ions was examined at 30°C, pH 7, and adsorbent dosage of 100 mg/mL. It is clear from Figs. 2 and 3 that the percentage of copper and nickel adsorption decreased with the increase in initial metal ion concentration, however the net adsorption capacity was higher at higher concentrations. Recently, Maneechakr and Karnjanakom [25] also reported same pattern of metal ion adsorption. Initial metal ion concentration generates the driving force to withstand the resistance to the mass transfer of adsorbate from stock solution to adsorbent surface. Increase in initial copper and nickel ion concentration

enhanced the interaction between metal ion and adsorbent. The percentage removal of copper ions was initially 95.26% for 25 mg/mL and 49.52% for 150 mg/mL concentration. The percentage removal of nickel ions was initially 94.35% for 25 mg/mL and 46.25% for 150 mg/mL. In both studies, non-activated husk had lesser efficiency in metal ions removal. The percentage removal of ions by different activated husk showed efficiency as $ZnCl_2$ > KOH > HNO_3 > nonactivated. Further, the $ZnCl_2$-activated husk samples were taken up for the studies.

3.2.2. Effect of pH and contact time

Adsorption process revealed as the contact time increases, and the adsorption efficiency increases for the three pH values until saturation is achieved. The percentage removal of ions showed higher efficiency percentage around 63.4%, 75.2%, 92.8%, and 84.1% for pH of 5, 6, 7, and 8, respectively (refer Fig. S2). The contact time was increased from 2 to 10 h, the adsorption efficiency has increased only by a slight margin at higher contact time. From 6 to 10 h at pH 7, the efficiency has increased very slowly, indicating that equilibrium has been achieved between the copper ions on the surface of the adsorbent and in the metal solution. The optimum contact time was chosen to be 8 h and not 10 h, despite 10 h showing a higher efficiency value of 92.8%. This shows that saturation has occurred, which means that the surface of the adsorbent (CH) cannot accommodate any more adsorbate (nickel ions) and that the nickel ions on the surface of adsorbent and in the solution has achieved equilibrium.

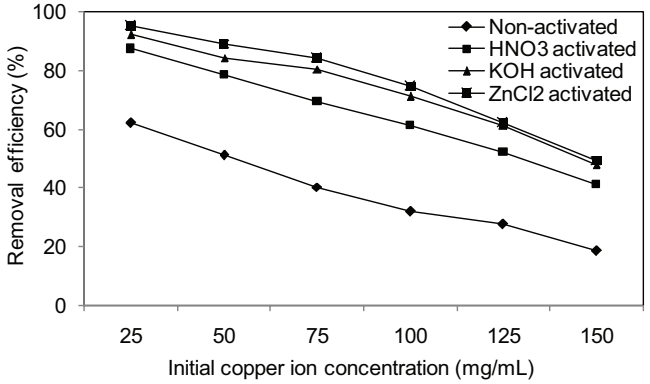

Fig. 2. Effect of initial copper metal ion concentration.

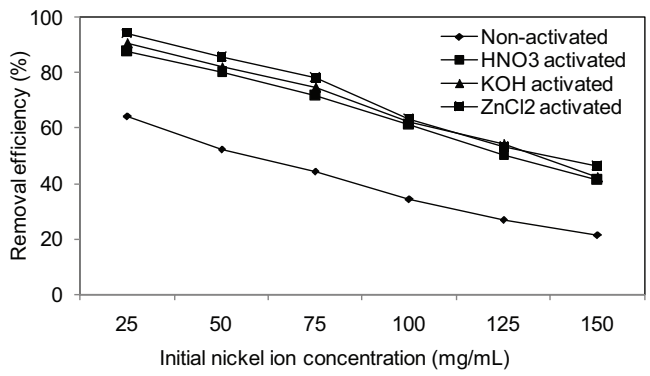

Fig. 3. Effect of initial nickel metal ion concentration.

Similarly for adsorption of copper ions, pH values ranging from 5 to 8 were chosen at contact times 2–10 h (refer Fig. S3). Compared with all the pH values, pH 7 shows very good results (89% efficiency in 6 h). Acidic pH range did not show promising results because at acidic pH, the amount of H^+ ions in the solution would increase, which may competitively bind to the surface of CH by impeding the adsorption of copper ions to the surface of adsorbent. Similar results were observed from the study conducted on Pb^{2+} and Hg^{2+} ions adsorption using Ti(IV) iodovanadate cation exchanger and alizarin red-S-loaded amberlite IRA-400 resin from aqueous medium [26,27]. From 6 to 10 h at pH 7, the efficiency has increased very slowly, indicating that equilibrium has been achieved between the copper ions on the surface of the adsorbent and in the metal solution. The optimum contact time was chosen to be 6 h and not 10 h, despite 10 h showing a higher efficiency value of 89.9%. Thus the shorter contact time was chosen, and later modifications would be carried out on the adsorbent to increase the efficiency at an even shorter period. Similar study conducted on copper and nickel removal using graft copolymer of glucose revealed optimum contact time as 4 h [28]. In contrast to this work, this study revealed the removal efficiency of more than 80% by 4 h contact time.

3.2.3. Effect of adsorbent dosage

Effect of adsorbent dosage on metal ion adsorption was conducted with different biosorbent dosage, from 100 to 500 mg/mL. Fig. 4 revealed that adsorbent dosage increases when the efficiency increases. It is also clear that because a very good result was obtained at 100 mg itself, not much difference is visible for the other increasing values of adsorbent dosage. This is because the metal ion concentration is kept constant at 75 mg/L, but the adsorbent dosage is increased, hence no significant adsorption is taking place. Biosorbent dose is an important parameter to estimate the amount of biosorbent material for the given initial metal ion concentration. The amount of available active sites for the biosorption process depends upon the amount of adsorbent during the adsorption process.

At higher biosorbent dosages, the presence of metal ions is inadequate to cover all the exchangeable sites on the biosorbent which provides fewer uptakes of metal ions onto the biosorbent. Further, it was observed that the percentage

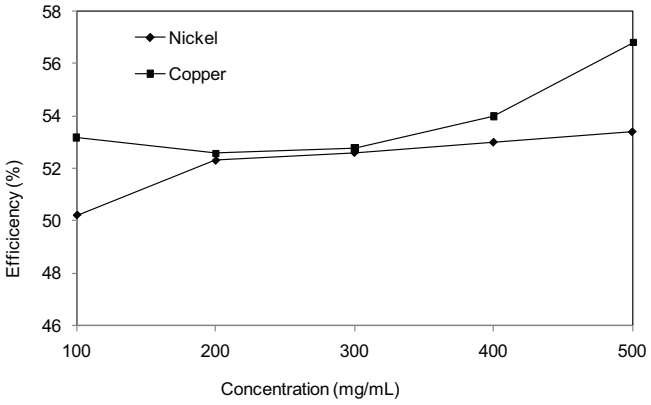

Fig. 4. Effect of adsorbent dosage.

removal of metal ions was increased with the increase in biosorbent dosage. The reason for the increase in percentage removal with increase in biosorbent dose was attributed to the increase in the number of available active sites with the increase in adsorbent dose, and this reaches a constant value finally which may be due to saturation of the sites [29].

3.2.4. Effect of temperature

Adsorption of nickel and copper ions was investigated as a function of temperature, and maximum removal of ions was at 40°C and 45°C, respectively. Fig. 5 explains the batch adsorption experiments performed at different temperatures (25°C, 30°C, 35°C, 40°C, 45°C, 50°C). The sorbates pyrolyzed at 40°C for 8 h shows 95.4% efficiency with nickel and at 45°C for 6 h showed 91.2% efficiency with copper, respectively. It is inferred that 40°C and 45°C are the ideal temperatures for adsorption studies for both copper and nickel because only at these temperatures the efficiency of adsorption is maximum.

Availability of active sites in the adsorbent material was increased for the adsorption, diffusion, and penetration of heavy metals [30]. However, increase in the temperature could affect the adsorption process, it was remarkably indicates that the biosorption is an exothermic process which means adsorption capacity is inversely proportional to the temperature, this might be due to the weakening of adsorptive forces between the active sites and the metal ions on the surface of the adsorbent material [31].

3.3. Desorption studies

Desorption of copper ions and their percentage efficiency was elaborated studied. For $ZnCl_2$-activated sample, the efficiency decreases from 89.24% (first wash) to 62.35% (third wash). Because the decrease in the percentage efficiency was not so drastic as other activated samples and on comparison of third wash, $ZnCl_2$ showed highest percentage efficiency it was considered to be a good regenerative sample (refer Fig. S4). From Fig. S5, it was interpreted that for $ZnCl_2$-activated sample, the efficiency decreases from 94.52% to 77.53%. Generally for regeneration studies, there should be a decrease of efficiency from first to third wash, which is seen in HCl-activated sample. Hence HCl-activated sample was found to be the best sample with regeneration capacity.

3.4. Recycling studies

In this study, the usage of adsorbent on metal ion removal from aqueous solution was studied. Though the removal efficiency is higher, it ultimately ends up in higher process cost. To overcome this, it is important to recover or reuse the spent adsorbent. In this study, reusability of the adsorbent was studied. Fig. 6 shows the reusability of catalyst after batch adsorption process. The removal efficiency was decreased in the recovered and reused adsorbent when compared with the initial batch process. Though the reduction in removal percentage is observed, it is promising in comparison within the cycle process. It was observed that maximum three to four times of adsorbent reusability is applicable and this in turn reduces the overall cost of the process.

3.5. Adsorption isotherms

Adsorption is a process that involves a solid phase and liquid or gas phase, the solid phase being the adsorbent and the liquid or gas phase being the adsorbate. The adsorbent displays a specific affinity toward the adsorbate which makes the adsorbate adhere to the surface of the adsorbent. This process continues until equilibrium is established between the adsorbate in the solution and the adsorbate on the surface of the adsorbent. Two parameter adsorption isotherm models (Freundlich and Langmuir isotherms) were used to investigate the adsorption rate of nickel and copper ions onto the adsorbent material. The Freundlich, Langmuir, Redlich, and Sips plots in their respective linear forms are shown in Figs. S6–S9.

For plotting the isotherms, an experiment was carried out where the adsorbent dosage was varied from 100 mg to 1 g, where the metal ion concentration, pH, contact time, and temperature were all kept constant. The parameter of these models such as Langmuir maximum adsorption capacity (q_m) and equilibrium constant (K_L), Freundlich equilibrium constant (K_F), correlation coefficient (R^2), and error values (sum of squared error [SSE] and root-mean-squared value [RMSE]) were examined by nonlinear regression analysis using MATLAB (R) curve fitting tool. Best-fitted adsorption isotherm model was identified using correlation coefficient values (R^2).

Table 2 elaborates the best-fitted values through the two-parameter isotherm system. The correlation coefficient

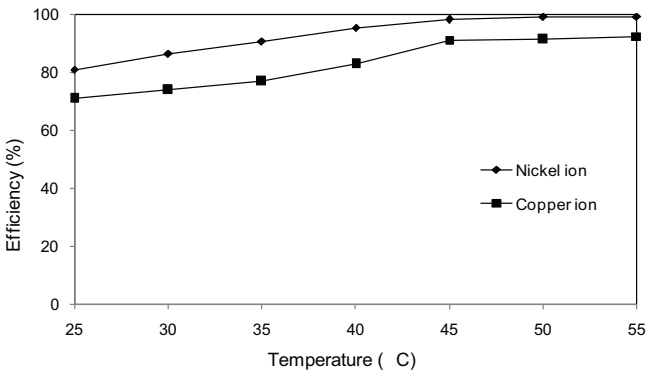

Fig. 5. Effect of temperature on adsorption.

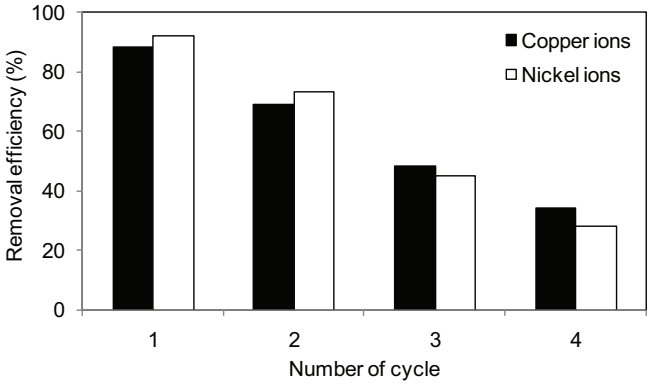

Fig. 6. Recyclability of adsorbent from batch studies.

Table 2
Parameters of Langmuir, Freundlich, Redlich–Peterson, and Sips isotherms evaluated from the linear plots

		Copper	Nickel
Langmuir plot	R^2	0.992	0.981
	q_{max} (mg/g)	66.33	131.2
	K_L (L/mg)	0.032	0.019
Freundlich plot	R^2	0.99	0.98
	N	1.166	1.112
	K_F (L/mg)	2.307	2.781
Redlich–Peterson	R^2	0.9877	0.9912
	K_{RP} (L/g)	0.365	0.439
	A	–18.9	–0.21
Sips	R^2	0.99	0.9916
	K_S (L/g)	0.209	0.2321
	A	0.043	0.027

values (R^2) showed higher values of 0.992 for copper and 0.981 for nickel for Langmuir plot when compared with Freundlich plot. The 'n' value from Freundlich plot is the degree of favorability, where an 'n' value between 1 and 10 is acceptable. The higher the n value, the stronger is the interaction between the adsorbent and adsorbate. Because the 'n' value for nickel is 1.112, it is lower in the range. Further, Freundlich plot for nickel is not highly favorable. Hence, Langmuir plot shows a better fit to the adsorption data for copper and nickel, compared with Freundlich plot. From the results, it was clear that the adsorbent surface was made up of heterogeneous patches which were constructive for adsorption mechanism.

3.6. Adsorption kinetic studies

The adsorption rates of metal ions in aqueous solutions to adsorbents were estimated using adsorption kinetics. Pseudo-first-order kinetic model [32] equation is as follows:

$$q_t = q_e(1 - \exp(-k_1 t)) \tag{8}$$

where k_1 is the pseudo-first-order kinetic rate constant (min^{-1}) and t is the time (min).

Pseudo-second-order kinetic model [33] equation is as follows:

$$q_t = \frac{q_e^2 k_2 t}{1 + q_e k_2 t} \tag{9}$$

where t is the time (min) and k_2 is the pseudo-second-order kinetic rate constant (g/mg min).

The Elovich kinetic model equation [34] as follows:

$$q_t = (1 + \beta_E)\ln(1 + \alpha_E \beta_E t) \tag{10}$$

where β_E (g mg^{-1}) denotes the desorption constant related to the activation energy of chemosorption and α_E is the initial adsorption rate (mg g^{-1} min^{-1}).

The Weber–Morris model equation [35] is as follows:

$$q_t = k_p t^{\frac{1}{2}} + c \tag{11}$$

where q_t is the adsorption rate at time t (mg g^{-1}), k_p is the intraparticle diffusion rate constant (mg g^{-1} $min^{-1/2}$), t is the time (min), and c is the intercept.

Generally, adsorption rate of metal ions will be high due to more number of active sites availability during the initial period, which tends to increase the concentration gradient between the metal ions in the solution and the surface of the adsorbent [36]. When the equilibrium time was increased to that of increase in initial metal ion concentrations, it generates a larger driving force to overcome all mass transfer resistances between the liquid and the solid phase [37].

The pseudo-first-order kinetics constant (k_1) and q_e, the pseudo-second-order kinetic constant (k_2) and q_e, and the parameters such as correlation coefficient values (R^2) and error values (SSE and RMSE), the Elovich kinetic model constant (α_E) and k_p the intraparticle diffusion rate (Weber and Morris) constant were determined by nonlinear regression analysis, using a MATLAB (R) curve fitting tool. Tables 3 and 4 elaborate the calculated parameters data for the copper and nickel ions.

The experimental results were used to recognize the best-fitted adsorption kinetic model. The calculated adsorption capacity (q_e, cal) values were compared with the experimental equilibrium adsorption capacity (q_e, exp) values of pseudo-first-order, pseudo-second-order, Elovich kinetic model, and Weber–Morris model of activated CH (refer Figs. S10–S17). The comparison statement clearly confirmed that the calculated adsorption capacity (q_e, cal) values of the Elovich kinetic model were closer to the experimental adsorption capacity (q_e, exp) values. The correlation coefficient values are 0.995, 0.99, 0.989, and 0.991 at 25, 50, 75, and 100 mg/L, respectively, for copper ions. Similarly, the correlation coefficient values are 0.983, 0.994, 0.976, and 0.972 at 25, 50, 75, and 100 mg/L, respectively, for nickel ions. The adsorption process involves chemisorptions mechanism, and the rate of site occupation is proportional to the square of the number of unoccupied sites. This result indicated that the Elovich kinetic is the best-fitted adsorption kinetic model for the adsorption of Ni and Cu ions from the aqueous solution onto the adsorbents.

3.7. Column studies

The adsorbent free beads exhibited negligible amount of metal ions removal efficiency when compared with the immobilized beads. This confirmed that the immobilizing material does not involve in any metal ion removal mechanism. The adsorption efficiency of adsorbent material and its behavior were studied using the batch experimental results. However, the batch adsorption experiment data could not give the scale-up data for industrial treatment systems, whereas continuous flow system (column) studies were normally employed for scale-up process [38]. Column adsorption studies are an effective process for

Table 3
Kinetic parameters for the adsorption of Cu ions onto coffee husk

Kinetic model	Parameters	Concentration of Cu ions (mg/L)			
		25	50	75	100
Pseudo-first order	K (min^{-1})	0.039	0.03149	0.02139	0.01254
	$q_{e,\ cal}$ (mg/g)	21.97	42.13	46.48	86.04
	R^2	0.983	0.9916	0.9768	0.9863
	SSE	5.68	9.63	46.48	38.11
	RMSE	1.376	1.792	3.936	3.564
Pseudo-second order	K (min^{-1})	0.00198	0.00067	0.00025	0.00007
	$q_{e,\ cal}$ (mg/g)	25.8	51.75	31.55	126.2
	R^2	0.9914	0.9969	0.9842	0.9891
	SSE	2.879	3.531	31.55	30.32
	RMSE	0.9796	1.085	3.243	3.179
Elovich kinetic model	α (mg/g/min)	0.2044	0.0276	0.0048	0.0007
	β (g/mg)	3.912	10.74	20.86	42.01
	R^2	0.9953	0.9991	0.9893	0.9915
	SSE	1.572	1.04	21.36	23.74
	RMSE	0.7239	0.588	2.669	2.813

Table 4
Kinetic parameters for the adsorption of Ni ions onto coffee husk

Kinetic model	Parameters	Concentration of Ni ions (mg/L)			
		25	50	75	100
Pseudo-first order	K (min^{-1})	0.03199	0.026	0.0157	0.0115
	$q_{e,\ cal}$ (mg/g)	22.4	42.34	66.34	89.83
	R^2	0.9792	0.9831	0.9646	0.9645
	SSE	6.9	18.54	70.86	99.29
	RMSE	1.517	2.486	4.86	5.753
Pseudo-second order	K (min^{-1})	0.00133	0.0005	0.00014	0.00006
	$q_{e,\ cal}$ (mg/g)	27.32	53.58	91.45	130.2
	R^2	0.9826	0.9905	0.9711	0.9687
	SSE	5.763	10.37	57.82	87.7
	RMSE	1.386	1.859	4.39	5.4
Elovich kinetic model	α (mg/g/min)	0.0652	0.014	0.0019	0.0007
	β (g/mg)	5.064	12.39	27.1	42.52
	R^2	0.9835	0.9948	0.9764	0.9726
	SSE	5.464	5.678	47.15	76.68
	RMSE	1.35	1.376	3.964	5.056

metal adsorption. Fig. 7 describes percentage efficiency and the types of beads at different time intervals conducted by continuous process. From the table, it can be inferred that there is a significant difference between the removal of copper and nickel by control, encapsulated, and hybrid beads.

Control beads showed copper removal efficiency around 29.07% and 30.47% at 30 and 60 min in continuous mode, respectively. For hybrid beads, the removal efficiency is 79.07% and 82.27% at 30 and 60 min for copper ions, respectively. For encapsulated beads, the removal efficiency 89.2% and 91.4% at 30 and 60 min, respectively. Compared with both encapsulated and hybrid beads, the former is more efficient than the latter in case of continuous studies.

In the case of nickel ions, control beads showed percentage removal from 32.50% to 35.42% from 30 and 60 min in continuous mode, respectively. For hybrid beads, the percentage removal increases 78.25% to 84.36% from 30 to 60 min, respectively. For encapsulated beads, the percentage removal increases 91.6% to 93.6% from 30 to 60 min, respectively. Comparing different beads efficiency, encapsulated beads showed higher efficiency than other beads.

3.7.1. Bed-depth service time model

The adsorption efficiency of the bed at different intervals was calculated using bed-depth service time (BDST) model (refer Fig. S18). The BDST model explains the dynamic

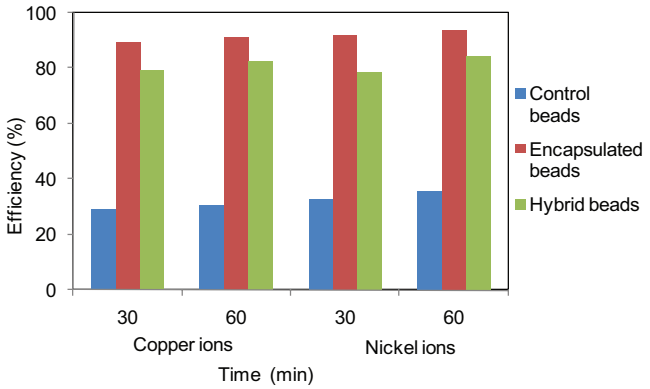

Fig. 7. Effect of various beads on metal ions adsorption.

behavior of column. The model also depicts the study adsorption process with limitations on internal and external diffusions. The graph was drawn between time (h) and bed height (cm) at a flow rate of 10 mL/min. The adsorption efficiency of bed per unit volume N_o was estimated from slope of BDST graph. The rate constant K_a was calculated from intercept of plot. The rate of solute transfer from the liquid phase to solid phase was calculated by rate constant K_a. The N_o was 525 mg/mL for nickel ions and 555 mg/mL for copper ions. The rate constant K_a was 0.00098 L/mg h for copper and 0.0014 L/mg h for nickel ions. The BDST model study helps in scaling process for flow rates without experimental runs. The adsorption capacity of metal ions was higher in column study than batch study due to higher concentration difference between the metal ions in liquid phase and adsorbent was in solid phase.

4. Conclusion

This study clearly indicates that CH can be used as a low-cost adsorbent for removal of heavy metals (copper and nickel). The chemical modification of adsorbent increased the efficiency of adsorption on adsorbent surface. It can be concluded that the CH modified with $ZnCl_2$ has high adsorption and regeneration efficiency for both copper and nickel adsorption. The operating parameters such as adsorbent dosage, contact time, pH, and initial metal ion concentration were depicted for metal ion adsorption efficiency. The maximum metal ion adsorption efficiency of CH was around 6 h contact time, 40°C temperature, pH 7, and 75 mg/mL of initial copper ion concentration. The adsorption isotherm studies were conducted by various isotherm models. Isotherm results shows that Langmuir fits the experimental data for both copper and nickel when compared with other models. The kinetic study revealed that the pseudo-first order was the best fit kinetic model. From the thermodynamic studies, it is observed that the adsorption process is less disordered and spontaneous in nature. From immobilization studies, we can interpret that continuous studies can be used depending on the industrial requirements. The column parameters such as initial metal ion concentration, bed height, and flow rate were optimized by BDST model. From the study, CH can be used as an effective economical biosorbent material for wastewater treatment.

References

[1] P.S. Kumar, C. Senthamarai, A. Durgadevi, Adsorption kinetics, mechanism, isotherm and thermodynamic analysis of copper ions onto the surface modified agricultural waste, Environ. Prog. Sustainable Energy, 33 (2014) 28–37.
[2] P. Rajkumar, P. Senthil Kumar, S. Dinesh Kirupha, T. Vidhyadevi, J. Nandhagopal, S. Sivanesan, Adsorption of Pb(II) ions onto surface modified *Guazuma ulmifolia* seeds and batch adsorber design, Environ. Prog. Sustainable Energy, 32 (2012) 307–316.
[3] L. Zheng, Z. Dang, C. Zhu, X. Yi, H. Zhang, C. Liu, Removal of cadmium(II) from aqueous solution by corn stalk graft copolymers, Bioresour. Technol., 101 (2010) 5820.
[4] D.W. O'Connell, C. Birkinshaw, T.F. O'Dwyer, Heavy metal adsorbents prepared from the modification of cellulose: a review, Bioresour. Technol., 99 (2008) 6709.
[5] L. Jarup, Hazards of heavy metal contamination, Br. Med. Bull., 68 (2003) 167–182.
[6] C. Jeon, J.H. Cha, Removal of nickel ions from industrial wastewater using immobilized sericite beads, J. Ind. Eng. Chem., 24 (2015) 107–112.
[7] M.A. Barakat, New trends in removing heavy metals from industrial wastewater, Arabian J. Chem., 4 (2011) 361–377.
[8] C.A. Basha, K. Ramanathan, R. Rajkumar, M. Mahalakshmi, P.S. Kumar, Management of chromium plating rinsewater using electrochemical ion exchange, Ind. Eng. Chem. Res., 47 (2008) 2279–2286.
[9] P.S. Kumar, S. Ramalingam, R.V. Abhinaya, K.V. Thiruvengadaravi, P. Baskaralingam, S. Sivanesan, Lead(II) adsorption onto sulphuric acid treated cashew nut shell, Sep. Sci. Technol., 46 (2011) 2436–2449.
[10] P.S. Kumar, Adsorption of lead(II) ions from simulated wastewater using natural waste: a kinetic, thermodynamic and equilibrium study, Environ. Prog. Sustainable Energy, 33 (2014) 55–64.
[11] Mu. Naushad, Z.A. ALOthman, M. Islam, Adsorption of cadmium ion using a new composite cation-exchanger polyaniline Sn(IV) silicate: kinetics, thermodynamic and isotherm studies, Int. J. Environ. Sci. Technol., 10 (2013) 567–578.
[12] Mu. Naushad, T. Ahamad, B.M. Al-Maswari, A. Abdullah Alqadami, S.M. Alshehri, Nickel ferrite bearing nitrogen-doped mesoporous carbon as efficient adsorbent for the removal of highly toxic metal ion from aqueous medium, Chem. Eng. J., 330 (2017) 1351–1360. doi: http://dx.doi.org/10.1016/j.cej.2017.08.079.
[13] A. Mittal, Mu. Naushad, G. Sharma, Z.A. ALOthman, S.M. Wabaidur, M. Alam, Fabrication of MWCNTs/ThO_2 nanocomposite and its adsorption behavior for the removal of Pb(II) metal from aqueous medium, Desal. Wat. Treat., 57 (2016) 21863–21869. doi: 10.1080/19443994.2015.1125805.
[14] Mu. Naushad, Z.A. ALOthman, M.M. Alam, Md. Rabiul Awual, G.E. Eldesoky, M. Islam, Synthesis of sodium dodecyl sulfate-supported nanocomposite cation exchanger: removal and recovery of Cu^{2+} from synthetic, pharmaceutical and alloy samples, J. Iran. Chem. Soc., 12 (2015) 1677–1686.
[15] A.A. Alqadami, Mu. Naushad, Z.A. ALOthman, A.A. Ghfar, Novel metal-organic framework (MOF) based composite material for the sequestration of U(VI) and Th(IV) metal ions from aqueous environment, ACS Appl. Mater. Interfaces, 9 (2017) 36026–36037.
[16] U.P. Kiruba, P.S. Kumar, C. Prabhakaran, V. Aditya, Characteristics of thermodynamic, isotherm, kinetic, mechanism and design equations for the analysis of adsorption in Cd(II) ions-surface modified Eucalyptus seeds system, J. Taiwan Inst. Chem. Eng., 45 (2014) 2957–2968.
[17] Mu. Naushad, M.R. Khan, Z.A. ALOthman, Ala'a H. Al-Muhtaseb, Md. Rabiul Awual, A.A. Alqadami, Water purification using cost effective material prepared from agricultural waste: kinetics, isotherms, and thermodynamic studies, Clean Soil Air Water, 44 (2016) 1036–1045.
[18] M. Ghasemi, M. Naushad, N. Ghasemi, Y. Khosravi-fard, Adsorption of Pb(II) from aqueous solution using new

adsorbents prepared from agricultural waste: adsorption isotherm and kinetic studies, J. Ind. Eng. Chem., 20 (2014) 2193–2199.
[19] Mu. Naushad, M.R. Khan, Z.A. ALOthman, I. AlSohaimi, F.R. Reinoso, T.M. Turki, R. Ali, Removal of BrO^{3-} from drinking water samples using newly developed agricultural waste-based activated carbon and its determination by ultra-performance liquid chromatography-mass spectrometry, Environ. Sci. Pollut. Res., 22 (2015) 15853–15865.
[20] ICO, Total Coffee Production of Exporting Countries, International Coffee Organization, London, UK, 2012.
[21] P.S. Murthy, M.M. Naidu, Sustainable management of coffee industry by-products and value addition: a review, Resour. Conserv. Recycl., 66 (2012) 45–58.
[22] N. Azouaou, Z. Sadaoui, A. Djaafri, H. Mokaddem, Adsorption of cadmium from aqueous solution onto untreated coffee grounds: equilibrium, kinetics and thermodynamics, J. Hazard. Mater., 184 (2010) 126–134.
[23] M.H. Baek, C.O. Ijagbemi, O. Se-Jin, D.S. Kim, Removal of malachite green from aqueous solution using degreased coffee bean, J. Hazard. Mater., 176 (2010) 820–828.
[24] S.K. Papageorgiou, F.K. Katsaros, E.P. Kouvelos, J.W. Nolan, H. Le Deit, N.K. Kanellopoulos, Heavy metal sorption by calcium alginate beads from *Laminaria digitata,* J Hazard. Mater., 137 (2006) 1765–1772.
[25] P. Maneechakr, S. Karnjanakom, Adsorption behaviour of Fe(II) and Cr(VI) on activated carbon: surface chemistry, isotherm, kinetic and thermodynamic studies, J. Chem. Thermodyn., 106 (2017) 104–112.
[26] Mu. Naushad, Z.A. ALOthman, Md. Rabiul Awual, M.M. Alam, G.E. Eldesoky, Adsorption kinetics, isotherms, and thermodynamic studies for the adsorption of Pb^{2+} and Hg^{2+} metal ions from aqueous medium using Ti(IV) iodovanadate cation exchanger, Ionics, 21 (2015) 2237–2245.
[27] Mu. Naushad, S. Vasudevan, G. Sharma, A. Kumar, Z.A. ALOthman, Adsorption kinetics, isotherms and thermodynamic studies for Hg^{2+} adsorption from aqueous medium using alizarin red-S-loaded amberlite IRA-400 resin, Desal. Wat. Treat., 57 (2016) 18551–18559.
[28] T. Hajeeth, T. Gomathi, P.N. Sudha, Adsorption of Copper (Ii) and Nickel (Ii) Ions from Metal Solution Using Graft Copolymer of Cellulose Extracted from the Sisal Fiber with Acrylonitrile Monomer, Advanced Nanomaterials and Emerging Engineering Technologies (ICANMEET), Chennai, 2013.
[29] S. Suganya, K. Kayalvizhi, P. Senthil Kumar, A. Saravanan, V. Vinoth Kumar, Biosorption of Pb(II), Ni(II) and Cr(VI) ions from aqueous solution using *Rhizoclonium tortuosum*: extended application to nickel plating industrial wastewater, Desal. Wat. Treat., 57 (2016) 25114–25139. doi: 10.1080/19443994.2016.1149111.
[30] L. Khezami, R. Capart, Removal of chromium(VI) from aqueous solution by activated carbons: kinetic and equilibrium studies, J. Hazard. Mater., 123 (2005) 223–231.
[31] A.S. Ozcan, S. Tunali, T. Akar, A. Ozcan, Biosorption of lead(II) ions onto waste biomass of *Phaseolus vulgaris* L.: estimation of the equilibrium, kinetic and thermodynamic parameters, Desalination, 244 (2009) 188–198.
[32] S. Lagergren, About the theory of so-called adsorption of soluble substances, Kungliga Svenska Vetensk Handl., 24 (1898) 1–39.
[33] Y.S. Ho, G. McKay, Pseudo-second order model for sorption processes, Process Biochem., 34 (1999) 451–465.
[34] M.J.D. Low, Kinetics of chemisorption of gases on solids, Chem. Rev., 60 (1960) 267–312.
[35] W.J. Weber, J.C. Morris, Kinetics of adsorption on carbon from solution, J. SaNit, Eng. Div. Am. Soc. Civil Eng., 89 (1963) 31.
[36] K. Vijayaraghavan, H.U.N. Winnie, R. Balasubramanian, Biosorption characteristics of crab shell particles for the removal of manganese(II) and zinc(II) from aqueous solutions, Desalination, 266 (2011) 195–200.
[37] K.K. Wong, C.K. Lee, K.S. Low, M.J. Haron, Removal of Cu and Pb from electroplating wastewater using tartaric acid modified rice husk, Process Biochem., 39 (2003) 437–445.
[38] M.M.M. Rahmatia, P. RabbaNi, A. Abdolali, A.R. Keshtkar, Kinetics and equilibrium studies on biosorption of cadmium, lead, and nickel ions from aqueous solutions by intact and chemically modified brown algae, J. Hazard. Mater., 185 (2011) 401–407.

Supplementary materials

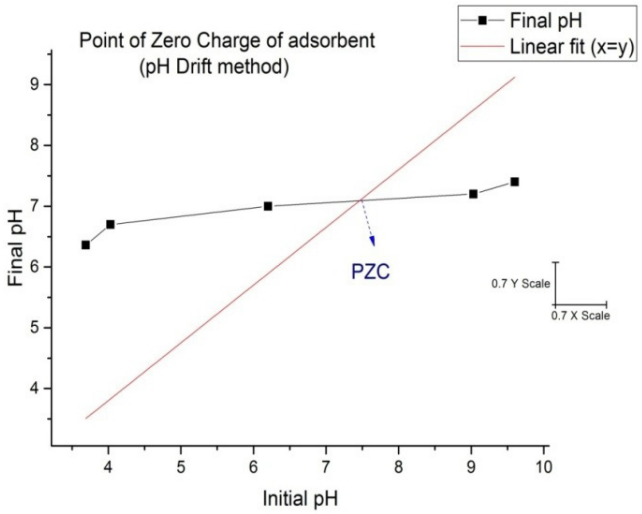

Fig. S1. Determination of PZC by pH drift method.

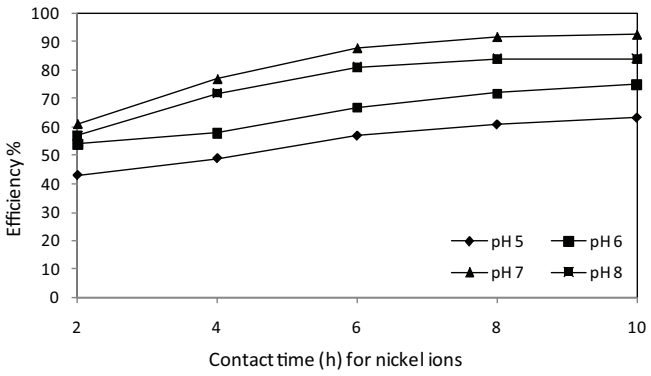

Fig. S2. Effect of contact time on nickel adsorption.

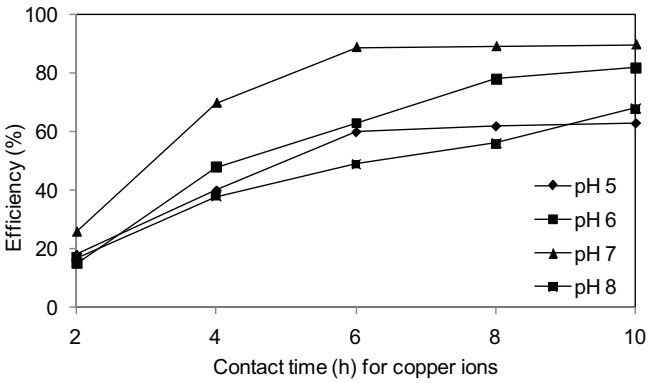

Fig. S3. Effect of contact time on copper adsorption.

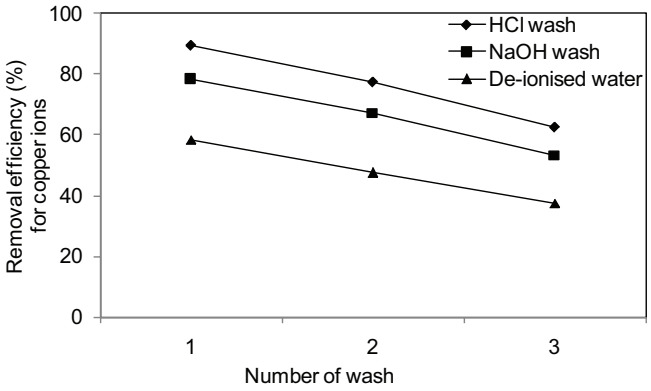

Fig. S4. Effect of desorption on copper ions.

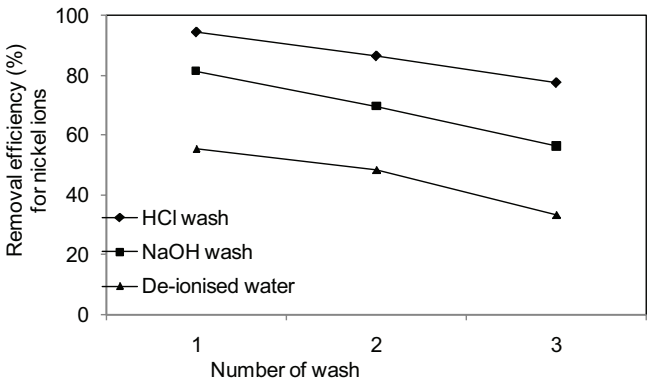

Fig. S5. Effect of desorption on nickel ions.

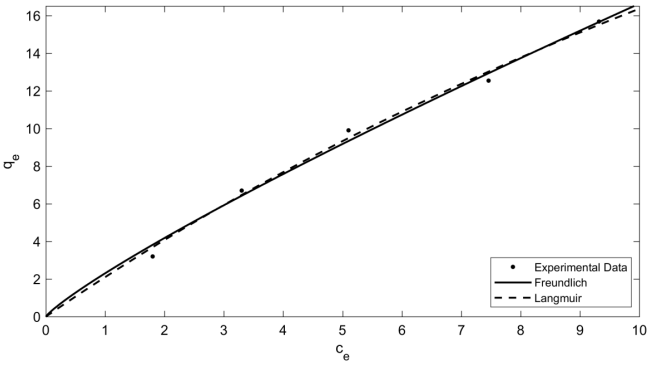

Fig. S6. Adsorption isotherm (Langmuir and Freundlich) of Cu ions.

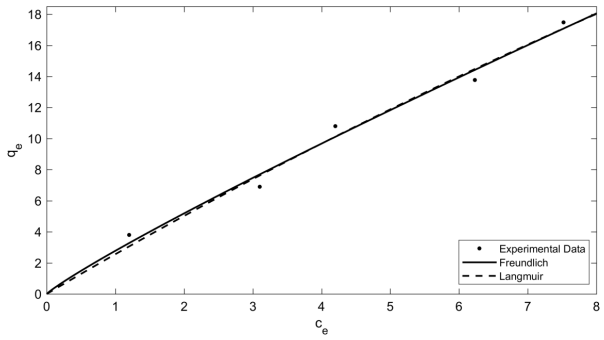

Fig. S7. Adsorption isotherm (Langmuir and Freundlich) of Ni ions.

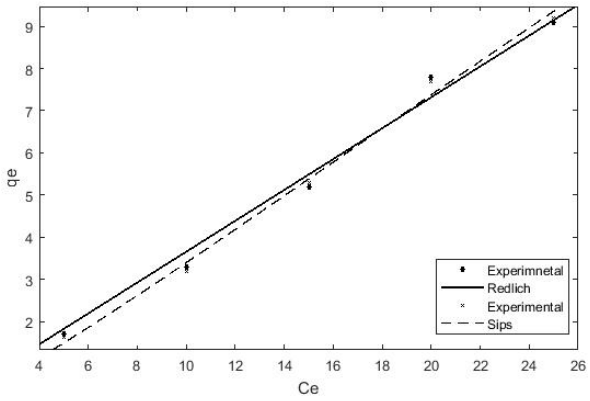

Fig. S8. Adsorption isotherm (Redlich and Sips) of Cu ions.

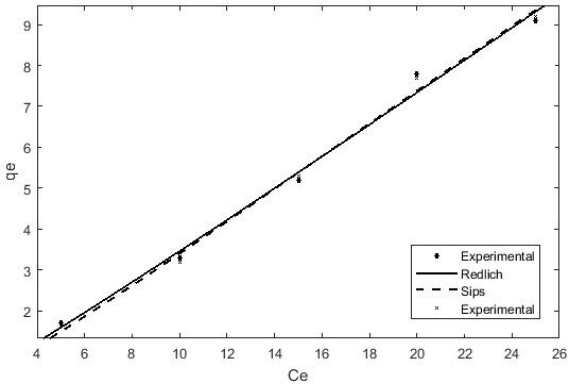

Fig. S9. Adsorption isotherm (Redlich and Sips) of Ni ions.

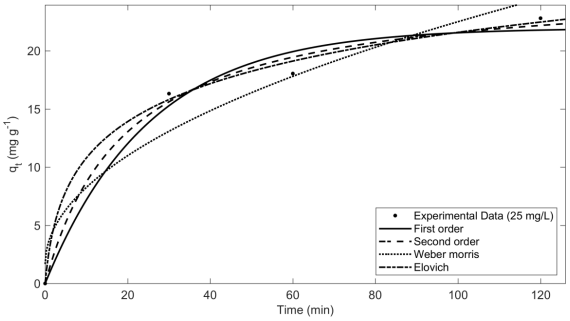

Fig. S10. Adsorption kinetic model fits for removal of copper ions (25 mg/mL).

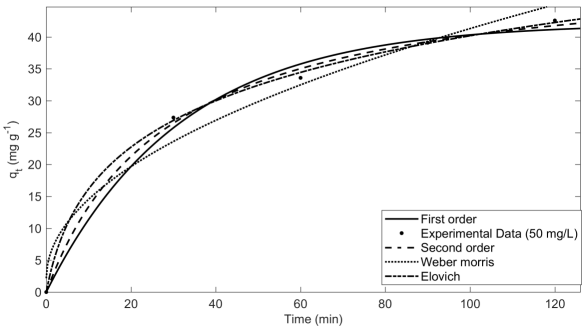

Fig. S11. Adsorption kinetic model fits for removal of copper ions (50 mg/mL).

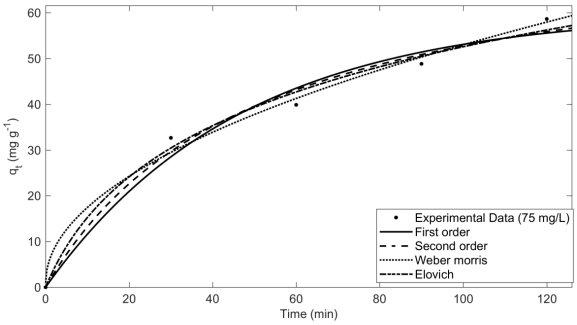

Fig. S12. Adsorption kinetic model fits for removal of copper ions (75 mg/mL).

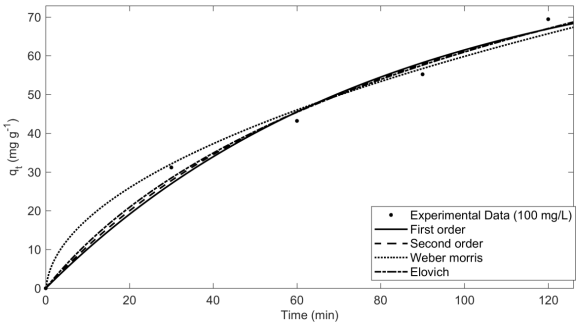

Fig. S13. Adsorption kinetic model fits for removal of copper ions (100 mg/mL).

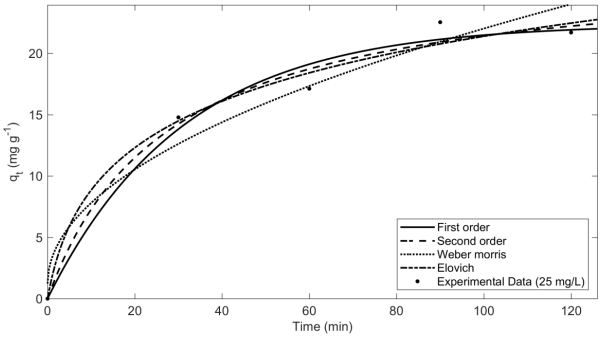

Fig. S14. Adsorption kinetic model fits for removal of nickel ions (25 mg/mL).

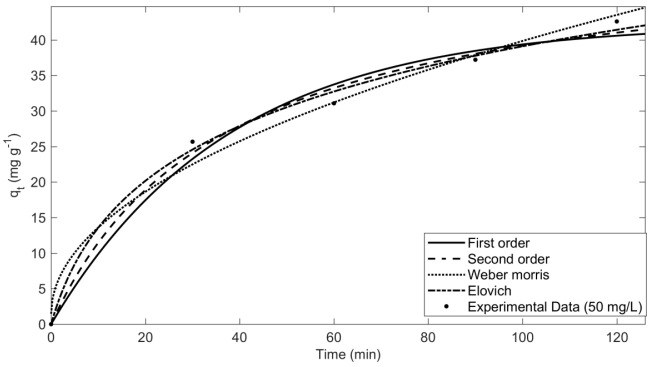

Fig. S15. Adsorption kinetic model fits for removal of nickel ions (50 mg/mL).

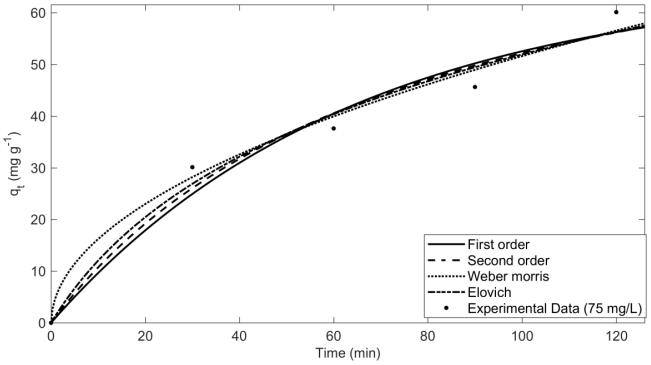

Fig. S16. Adsorption kinetic model fits for removal of nickel ions (75 mg/mL).

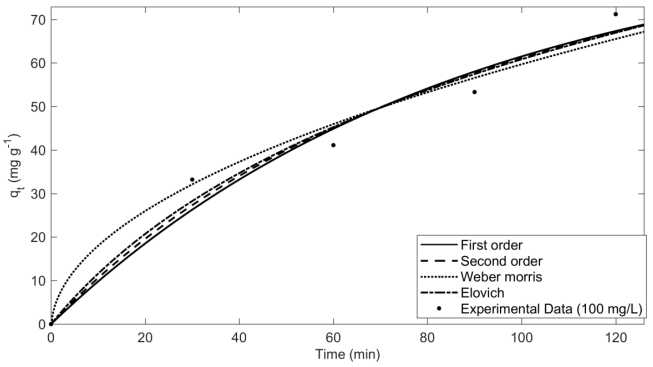

Fig. S17. Adsorption kinetic model fits for removal of nickel ions (100 mg/mL).

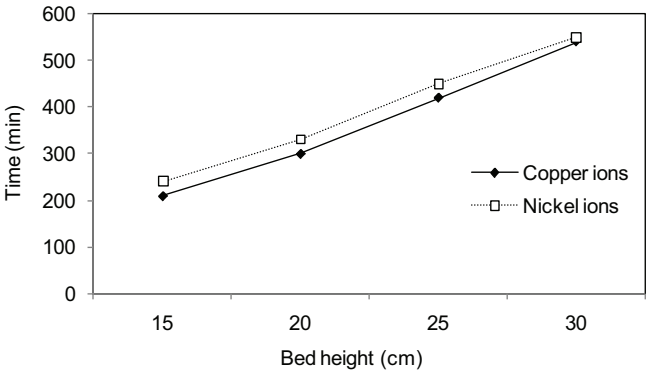

Fig. S18. BDST model plot for the removal of metal ions.